Case Study

Characterization and Geotechnical Investigations of a Riverbank Failure in Florence, Italy, UNESCO World Heritage Site

S. Morelli, Ph.D.[1]; V. Pazzi, Ph.D.[2]; L. Tanteri[3]; M. Nocentini[4]; L. Lombardi[5]; G. Gigli[6]; V. Tofani[7]; and N. Casagli[8]

Abstract: On May 25, 2016, an artificial riverbank of the Arno River collapsed just upstream from the famous Ponte Vecchio bridge in the city of Florence, Italy, a UNESCO World Heritage Site. An analysis of the failure was performed to identify the damage condition of the involved structures, to define the causes of the failure, and preserve the site. This study was based on borehole integration and geotechnical characterization, terrestrial laser scanner (TLS) and digital photogrammetry (DP), bathymetric and geophysical surveys, riverbank stability analysis, and wall seismic vibrations assessment. The TLS survey results were used to characterize the three-dimensional (3D) wall deformations pattern, the landslide geometry, and to define the involved volumes. The riverbank stability analysis demonstrates that the lower safety factor was obtained in the case of complete saturation of filling materials and low river level in accordance with the major cause of collapse being attributed to the loss of water from subterranean pipes. **DOI: 10.1061/(ASCE)GT.1943-5606.0002305.**

Author keywords: Riverbank instability; Landslide characterization; Cultural heritage conservation; Geophysical investigation; Terrestrial laser scanner; Digital photogrammetry.

Introduction

The historic center of Florence, Italy, was added to the World Heritage List (WHL) of UNESCO in 1982. The first UNESCO World Heritage List was established in 1972 under the World Heritage Convention and encompassed several cultural and natural heritage sites worldwide for which assistance operations can be considered a priority for their conservation (UNESCO 1972).

The Tuscan city became a symbol of the Renaissance during the early Medici period (between the fifteenth and the sixteenth centuries), reaching extraordinary levels of economic and cultural development. The present historic center covers 5.05 km^2 and is bounded by the remains of the city's fourteenth-century walls. During its history, the historic center of Florence has suffered many geohydrological disasters, such as floods, landslides, and riverbank failures. Among all, the following events are worthy of mention: (1) the November 4, 1966, flood of the Arno River in Florence that killed 18 people and damaged or destroyed millions of art masterpieces and rare books (De Zolt et al. 2006), and (2) the slope instabilities of San Miniato Hill's northern slope in the historic city center of Florence documented and studied since the Renaissance (Fanti et al. 2006). Several monuments in the area, in fact, have been repeatedly damaged by the presence of what has historically been interpreted as a large, slow-moving landslide (Fanti et al. 2006).

The impact of geohydrological hazards on cultural heritages represents a multidisciplinary theme, which requires several different approaches (Canuti et al. 2009). A complete analysis involves geotechnical, structural, and engineering issues and can lead to the design of adequate countermeasures (Fanti et al. 2013). In literature, there are many examples of integrated approaches based on different survey and monitoring techniques for the study and conservation of cultural heritage sites affected by geohydrological hazards (Margottini and Spizzichino 2014; De Finis et al. 2017; Themistocleous et al. 2018). In particular, remote-sensing technologies are increasingly becoming useful tools for the onsite preservation of cultural heritage and are used to constantly update the condition report of a monument (Tapete et al. 2013; Themistocleous et al. 2015; Chen et al. 2018).

In this study, an integrated approach for the characterization of a riverbank failure of the Arno River in the historical center of Florence is presented. On May 25, 2016, a portion of the artificially built riverbank collapsed just a few meters from the famous Ponte Vecchio bridge, endangering the stability of a wider portion of the historic heritage site. In this research, a detailed study of this event is performed based on the integration of geotechnical characterization, remote sensing techniques, stability analyses, and geophysical

[1]Ph.D. Researcher, Dept. of Earth Sciences, Univ. of Florence, Via G. La Pira 4, Florence 50121, Italy.
[2]Ph.D. Researcher, Dept. of Earth Sciences, Univ. of Florence, Via G. La Pira 4, Florence 50121, Italy. ORCID: https://orcid.org/0000-0002-9191-0346
[3]Technician of the Center for Civil Protection, Dept. of Earth Sciences, Univ. of Florence, Largo E. Fermi, 2, Florence 50125, Italy. ORCID: https://orcid.org/0000-0002-0572-0096
[4]Director of the Center for Civil Protection,, Dept. of Earth Sciences, Univ. of Florence, Largo E. Fermi, 2, Florence 50125, Italy.
[5]Academic Technician, Dept. of Earth Sciences, Univ. of Florence, Via G. La Pira 4, Florence 50121, Italy.
[6]Associate Professor, Dept. of Earth Sciences, Univ. of Florence, Via G. La Pira 4, Florence 50121, Italy.
[7]Associate Professor, Dept. of Earth Sciences, Univ. of Florence, Via G. La Pira 4, Florence 50121, Italy (corresponding author). ORCID: https://orcid.org/0000-0003-2622-2034. Email: veronica.tofani@unifi.it
[8]Full Professor, Dept. of Earth Sciences, Univ. of Florence, Via G. La Pira 4, Florence 50121, Italy. ORCID: https://orcid.org/0000-0002-8684-7848

Note. This manuscript was submitted on June 3, 2019; approved on March 6, 2020; published online on July 16, 2020. Discussion period open until December 16, 2020; separate discussions must be submitted for individual papers. This paper is part of the ***Journal of Geotechnical and Geoenvironmental Engineering***, © ASCE, ISSN 1090-0241.

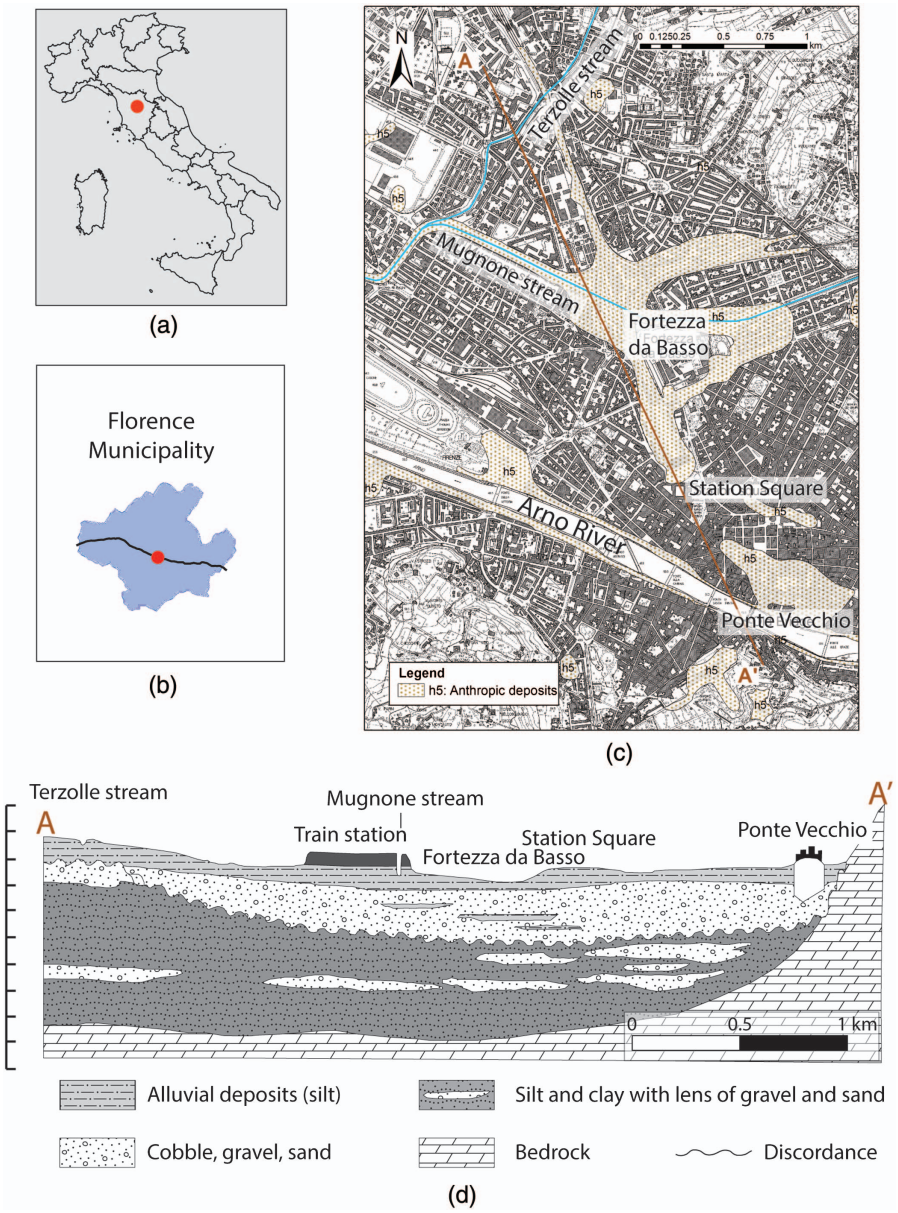

Fig. 1. (Color) Study area: (a) geographical framework, red dot is Florence; (b) Florence municipality, red dot is Florence city center; (c) distribution of current urban structure of Florence with distribution of main anthropic deposits and section line in which stratigraphy of plain is extracted (map data from Geoscopio 2013); and (d) geological reconstruction along section A–A′ of Fig. 1(c) according to Boccaletti et al. (1997).

surveys with the final aim of defining the damages of the involved structures, identifying the causes of the failure, recognizing the measures to manage the risk, and preserving and restoring the site.

Study Area

Geological and Geomorphological Evolution from Pliocene to Present

The city of Florence is crossed by the Arno River, which originates from a source in the southern slopes of Mt. Falterona (1,358 m above sea level) and, after 241 km, flows into the Thyrrenian Sea at Marina di Pisa. Its basin has an extension of approximately 8,830 km^2 and consists of flat plains (17% of the total surface), low mountain areas (15%), and hills/piedmont areas (68%) (Cencetti and Tacconi 2005). Due to its geological conformation, the Arno River crosses a variety of geomorphological landscapes, sequentially alternating hilly regions and alluvial plains, such as the Firenze-Prato-Pistoia Plain, where the metropolitan area of Florence is located (Morelli et al. 2012). This is a northwest-southeast oriented intermontane basin that is 45 km long and 10 km wide, with an average altitude of 45 m above sea level (Capecchi et al. 1975) (Fig. 1). It is delimited by two ridges (geologically represented by two horsts) mainly constituted by calcareous-marly flysch associated with ophiolites and arenaceous flysch (Abbate and Sagri 1970; Boccaletti and Colicartographers 1982; Pandeli 2008). The northern limit of the plain is marked by a normal fault that makes the basin a half-graben (Coli and Rubellini 2007).

The geomorphology in the area is closely connected to the lithology given that reliefs are mainly located at the aforementioned flysch outcrop. Gentler slopes (as in the hills south of the Arno River) are mostly associated with flysch of marly arenaceous composition, while loose lacustrine and fluvial sediments form

piedmont areas (Coli and Rubellini 2007). From a stratigraphic point of view, deposits older than the basin itself (3.2 million years) are only occasionally found through borehole investigations. The genesis of the half-graben is associated with the sedimentation of clay, sandy clay, and peat relatable to a lacustrine-swampy environment (Capecchi et al. 1975;Briganti et al. 2003). The presence of an ancient lake was already suggested in previous centuries by personalities of the caliber of Giovanni Villani, Leonardo da Vinci, and Giovanni Targioni Tozzetti (Pandeli 2008). Locally, these deposits give way to gravel produced by deltas of the torrents flowing into the lake.

During its history, the Arno most often occupied the southern part of the plain, as it currently does (Fig. 1). The modern construction of dams and the excavation of sediments from the riverbed (occurred especially during the postwar urban growth) caused a deepening of the river of approximately 6 m with consequential regressive erosion of its tributaries (Canuti et al. 1994; Rinaldi 1996). Such tributaries (except for Mugnone Creek) are geologically recent, as they date back to the activation of the fault that formed the Firenze-Prato-Pistoia half-graben. They are short, linear, and relatively steep. Today, they are mostly covered by the urban territory given recent city growth and are constrained underground, e.g., Fosso della Carraia, a small and almost entirely covered creek that flows into Arno River upstream of Lungarno Torrigiani (Morelli et al. 2014).

Riverbank

The current riverbank morphology is the result of urbanization typical of centuries-old cities, which have mainly developed along the rivers to exploit the waterpower; during their history, these cities have increasingly gained spaces at the expense of the fluvial area through the reduction of its section (Morelli et al. 2012). The current structure of the study area is the product of a specific urban redevelopment approved in 1866 and completed in 1872 in the overall framework of the reorganization that the city was experiencing during the years in which it was designated as the capital of Italy (1865–1871; Poggi 1882).

With a purely artificial nature and unique arrangement, the existing structure completely covers an area that, until the time of construction, was occupied by the left side of the riverbed, remaining almost unchanged since its origins [Fig. 2(a)]. In fact, it underwent only minimal conservation works overtime (Paolini 2014). Its structure [Fig. 2(b)] is composed as follows: (1) a vertical stone masonry retaining wall anchored directly to the substrate of the riverbed with four rows of piles; (2) a brick parapet (1.20-m high on average from the road surface), which is the continuation upward of the stone wall with the dual function of both protecting people from tumbling into the river and is used to avoid overflowing during the very high levels of floods, thus acting as a small levee wall (this is the only component here that suffered damages from floods); and (3) filling material and buried subservices between the stone wall and the original riverbank covered by a paved road.

The filling operation was mainly managed with compacted landfill and completed with the insertion of an arched vault culvert just adjacent to the buildings' foundations (reshaping the old morphology). Such handiwork, which is easily inspectable for its metric dimensions and completely isolated from the external terrain [Figs. 2(c and d)], operated in conjunction with a lifting water station of a coeval aqueduct system that was built approximately 600 m upstream. It was designed to give back to the river the amount of water that was captured to operate the pumps' turbines after the jump produced by the weir, and its outlet was located just upstream of Ponte Vecchio (a few meters downstream of the riverbank landslide). At the time of the landslide, the Lungarno Torrigiani (open to vehicular transit) housed a line of parking, a modern-era aqueduct pipe a few centimeters below the surface, and a retaining wall on the riverside partially covered by climbing plants, such as ivy and other plants, that are resistant to different degrees of humidity.

The Instabilities of Previous Riverbanks

Given the high urban development of the city during the centuries, several damaging inundations were repeatedly recorded; in some

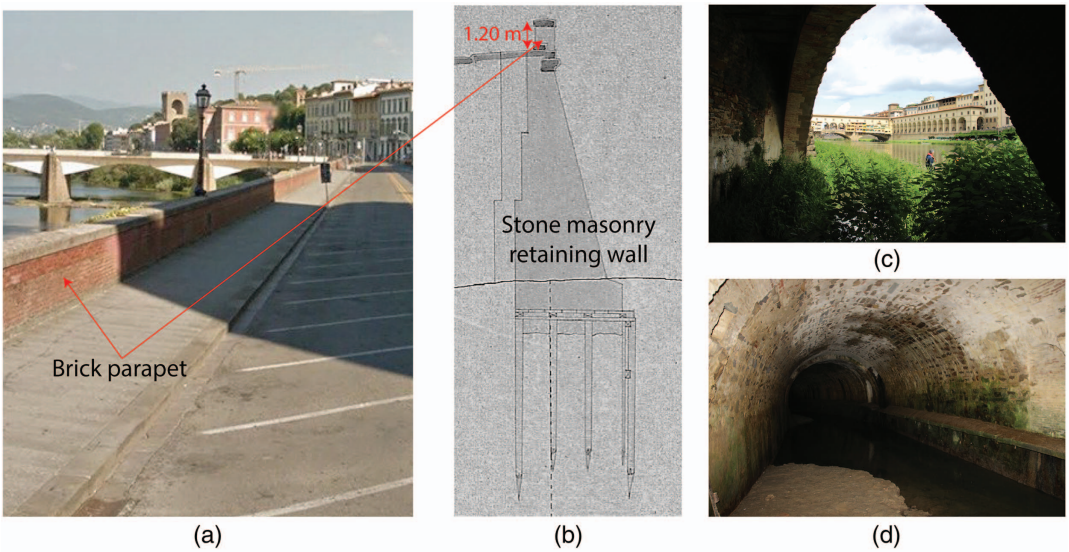

Fig. 2. (Color) Torrigiani riverbank embankment: (a) walkable floor condition of riverbank before 2016 collapse (image by S. Morelli); (b) retaining wall from original design drawings; (c) culvert internal development within riverbank seen from outlet as visible in 2017 (image by G. Gigli); and (d) outlet of arched vault culvert (image by G. Gigli).

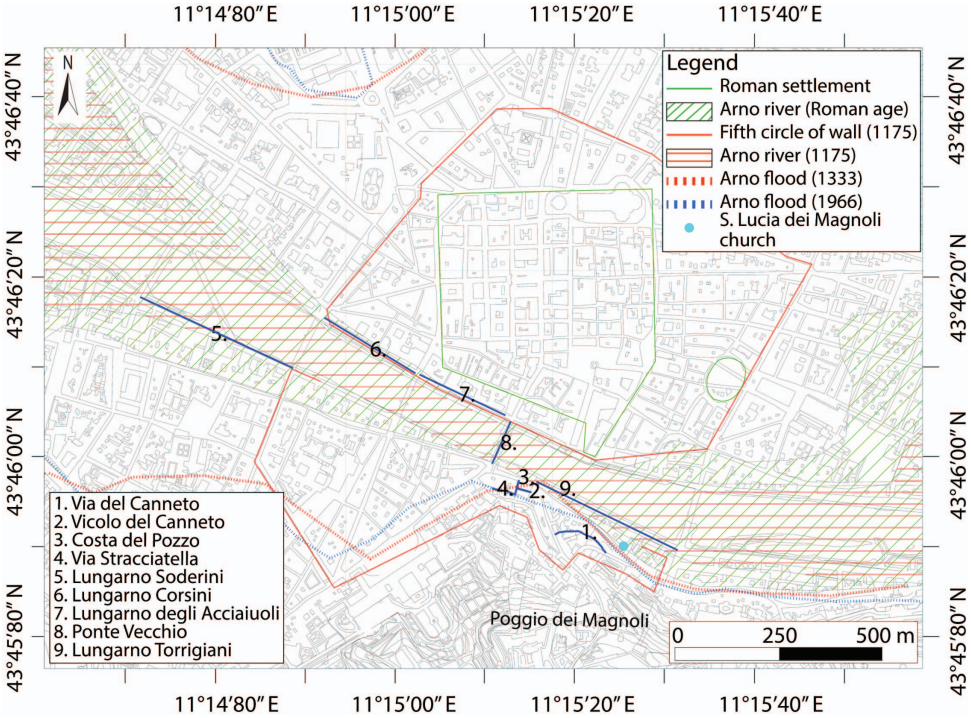

Fig. 3. (Color) Area with green diagonal hatches is Arno River during Roman age and green continuous line is original nucleus of Roman settlement. Area with red horizontal hatches is Arno River during twelfth century, and red continuous line is urban wall in 1,175 after enlargement of Roman city walls to include Arno River for first time in urban development. Dashed red and blue lines represent extension of floods in 1,333 and 1,966, respectively. Numbers 1–4 show some streets with name related to presence of water in history of city; numbers 5–7 show some streets parallel to Arno River (along riverbanks) that collapsed in previous times; numbers 8 and 9 are Ponte Vecchio and riverbank that collapsed on May 25, 2016, respectively. Base map is Regional Cartographic Topography. (Map data from Geoscopio 2013.)

cases, riverbank collapses and/or damages to structures and buildings directly facing the riversides were induced by turbulent flows (Canfarini 1978; Frati 2015) [Fig. 3(a)]. Collapses that occurred in the contemporary age instead had a greater emphasis not only because they are closer in time or were evaluated objectively more catastrophic in relation to the impacted urban agglomeration but also because a greater awareness of the high artistic and historical heritage value has gradually developed in peoples' consciousness (Guidoboni and Ferrari 1995), even going beyond the city limits. At the end of the nineteenth century, following the laying of an extensive and modern network of water supply beneath the urban area (Scampoli 2010), the risk of the riverbank instability was further enhanced by the threatening effects of uncontrolled water leaks and spills from the piping system installed just within the urbanized riverbanks. The maintenance of old structures, in fact, was not always regular, and a scarce natural dissipation of pore pressures was increasingly favored by the presence of vertical underground structures (underground passages, buried channels, sewer systems, foundations, and riverbank retaining walls) that contributed to the obstruction of the natural groundwater circulation. In recent decades, the maintenance of such a complex subterranean system was not always prompt and effective, and it occasionally induced criticalities for the health and security of citizens in different areas of the city (Morelli et al. 2014).

On July 4, 1965, a portion of the embankment along the Lungarno Soderini (left riverbank) rapidly collapsed (photo available online) within the Arno River after an unquantifiable leakage from the subterranean water supply network that hugely saturated the soil. Such an event engulfed the retaining wall, which was vertically built (as in the rest of the city) to protect the anthropic riverbank from high flood currents and to sustain the levee wall (masonry parapet). The resulting landslide had a volume of approximately 4,000–5,000 m^3 and a length and a width of 40 and 6 m, respectively. The landslide caused the death of one person. However, more casualties were also likely given that a very central area of the city was involved.

Following the collapse, the municipality conducted some site inspections to evaluate the stability of the Arno riverbanks, and many critical issues emerged both upstream and downstream of the affected area. The reconstruction works lasted for approximately four months. These works were so effectively reconstructed that the most disastrous flood of the twentieth century (November 4, 1966) occurred only one year after the completion of the reconstruction work without causing significant damages in the surrounding historical heritage and citizens as in other areas of the city. The chronicles report that at 7:00 a.m., a large and powerful mass of liquid reached just upstream of this embankment, then began to overflow and expand in all low-lying areas, including the 1965 readjusted riverbank and the entire riverside up to the 2016 collapsed sector (Catenacci 1992). However, the flood dynamics did not cause any significant collapses or structural damages capable of inducing a subsequent instability in the following days. Only minor damages to the street furniture or artefacts overlooking the watercourse (e.g., laceration and eradication of levee summits, retaining walls, and parapets) were recorded, and these damages were similar to other points of the urban perifluvial area (Canfarini 1978). At the same critical times, on the right riverbank, a portion of Lungarno degli Acciaiuoli embankment collapsed (photo available online from the newspapers of that year) due to the erosive strength of the river current for long stretches. Even the adjacent Lungarno Corsini embankment sustained slope failures, contributing to the rapid invasion of turbulent waters toward the inner areas of the city (Catenacci 1992).

Fig. 4. (Color) Photos show (a) roadway and moved retaining wall immediately after removal of vehicles stuck inside landslide; (b) repair of big pipeline affected from catastrophic failure; and (c and d) construction site setup stage (notice large tarps for temporary protection). (Images by M. Nocentini.)

2016 Riverbank Failure

Late on the night of May 24, 2016, a large amount of circulating surface water was observed in the Lungarno Torrigiani road by the residents despite the dry weather and the absence of rain. Due to the increase of surficial circulating water, at 4 a.m. on May 25, the local police recommended the authorities of the Florence Municipality to close the Lungarno Torrigiani for safety reasons. Simultaneously, the aqueduct company observed a decrease in the water pressure within an ND 600 pipeline of the plant. Following these events, the aqueduct manager activated a series of operations aimed at decreasing the leak of water from the pipeline (viz., reduction of the pressure in the water supply network of the town). At approximately 6 a.m., part of the Lungarno Torrigiani road surface collapsed with approximately 4 m in height and 150 m in breadth [Fig. 4(a)] via partial sliding of the underlying terrigenous layers toward the riverbed, causing a cusp-shaped deformation of the retaining wall without any shattering or toppling [Figs. 4(b, c, and d)]. This new collapse left the involved urban area without stable protection from Arno River dynamics and slope evolution.

After the landslide event, the stuck cars and the stagnant water were removed and two lines of action were simultaneously activated: (1) the construction of a pipeline bypass in correspondence with the broken one [Fig. 4(b)]; and (2) the subsoil investigation and characterization for the design of the reconstruction project in the area. Since the event could naturally extend even to the nearby areas, thereby increasing the damage to the heritage site and endangering the lives of workers involved in the construction sites, the Earth Science Department of the University of Florence was mobilized in coordination with the city authorities on the morning of May 25, 2016, to monitor the stability of the entire area. Therefore, an integrated monitoring system was installed to detect any real-time deformation of the masonry embankment wall in the collapsed area and the buildings in the surrounding area. The monitoring system was composed of the following devices/equipment (Fig. 5): (1) one robotic total station (RTS) with 18 targets; (2) one ground-based interferometric synthetic aperture radar (GB-InSAR); (3) one high performance long-range (3D) terrestrial laser scanner (TLS); (4) nine biaxial tiltmeters; (5) four crackmeters; and (6) three seismic ground motion stations.

Given the need to make the monitoring system immediately operational, remote instruments able to measure deformations from a station in the opposite bank were installed first (points 1–3), starting with the GB-InSAR (Tarchi et al. 1999; Casagli et al. 2017a, b, 2018)

Fig. 5. (Color) (a) Satellite image of study area with location of techniques employed to characterize Lungarno Torrigiani landslide: boreholes and downholes (red dots), TLS point of acquisition (yellow triangle), bathymetric survey extent of riverbed (blue dashed line), single-station seismic noise (H/V measures, green dots), and 3D electrical resistivity tomographies (3D-ERT) (map data © 2020 Google); (b) picture of GB-InSAR, TLS, and RTS positioning (image by L. Lombardi); (c) GB-InSAR targeted points over a colored point cloud of whole area obtained with TLS; and (d) front view of landslide area delimited by outermost fractures trace (white lines) with location of RTS targeted points, tiltmeters, crackmeters, and seismic stations (image by L. Lombardi).

because it uses natural reflectors already existing on the investigated scene and then continuing with the others. Once this part was optimized, in the following few days, the instruments more oriented to the local measurements (points 4 and 5) were installed directly in some specific sites of the observed area based on the interpretation of the first data. In addition, the seismic stations within the construction site accompanied all the executed works. The information coming from the sensors was received by a web platform in which the data were stored, elaborated, and made available for real-time warnings, viewing, and analysis. The results of the monitoring system are not presented in this paper due to space limitations, and this paper is focused mainly on the characterization of the mechanism and the evaluation of wall cracks for the restoration works.

Methodology

Failure Characterization

The following methods were integrated to characterize the failure (Fig. 5): boreholes and geotechnical laboratory tests (Morelli et al. 2010, 2017; Bicocchi et al. 2019), TLS (Gigli et al. 2012) of the subaerial riverbank and bathymetric survey of the frontal riverbed (Pazzi et al. 2016a), electrical resistivity topographies (ERTs) (Travelletti and Malet 2012; Pazzi et al. 2016c), and downholes (DH) and single-station seismic noise (SN) measurement (Spizzichino et al. 2013; Pazzi et al. 2017c). The data obtained from these techniques were used to perform the limit equilibrium stability analysis of the slopes.

Boreholes and Geotechnical Characterization

To reconstruct the lithological sequence and define the geotechnical characteristics of the materials involved in the failure, two exploratory boreholes were initiated until reaching a depth of 25 m (Fig. 5). The boreholes have highlighted a three-layer stratigraphy constituted by the following starting from the ground level; (1) filling materials, (2) alluvial deposits, and (3) shales with marls and argillaceous marls (Sillano Formation). The thicknesses of filling material and alluvial deposits are different in two boreholes. The filling material has a thickness ranging from 7.5 to 8.0 m, while the alluvial deposits have a thickness ranging from 2.0 to 4.0 m. Below the alluvial deposits, the Sillano Formation can be seen until the bottom of the borehole. Twenty samples were collected and analyzed from several boreholes and open pits excavated in the

Table 1. Geotechnical parameters obtained by laboratory tests and downhole surveys. The ranges of the downhole survey results are from two downhole surveys. The laboratory test results were used in the stability analysis of the slopes

Method	Properties/parameters	Filling material	Alluvial deposits	Sillano substrata	Interspace	Boxing
Laboratory tests	GF (%)	39	34	8	—	—
	SF (%)	43	31	38	—	—
	MF (%)	16	27	41	—	—
	CF (%)	2	8	13	—	—
	USCS classification	SM	SM	ML	—	—
	W_L (%)	22	27	26	—	—
	W_P (%)	17	18	18	—	—
	Ip (%)	5	9	8	—	—
	γ (kN/m^3)	17.6	19	20	—	—
	φ' (degrees)	26	35	26	—	—
	c′ (kPa)	0	0	10	—	—
Downhole survey	γ (kN/m^3)	17.00–17.15	17.72–17.88	20.27–21.24	—	—
	Vp (m/s)	500–573	861–941	2,137–2,620	—	—
	Vs (m/s)	95–116	459–562	693–834	—	—
	v	0.47–0.49	0.22–0.30	0.44	—	—
Slope stability analysis	γ (kN/m^3)	—	—	—	19	20
	φ' (degrees)	—	—	—	33	40
	c′ (kPa)	—	—	—	0	0

construction site soil (eight for the filling material, seven for the alluvial deposits, and five for the Sillano Formation).

Laboratory tests were conducted to determine grain size distributions, Atterberg limits, and soil unit weight (Pazzi et al. 2017c; Tofani et al. 2017; Bicocchi et al. 2019) for the different three layers (Table 1). Tests were performed following the ASTM recommendations (ASTM 1998, 2007, 2010). The shear strength of the soils was obtained via direct shear tests performed on remolded samples of the three layers of material using the direct shear box. The test was performed in saturated conditions. Effective shear strength parameters (effective cohesion c' and friction angle φ') were determined applying three different normal stresses (50, 100, and 150 kPa). The shear phase of the test was performed by applying a velocity of deformation defined via the consolidation phase results to provide drained conditions and to avoid the formation of excess pore water pressure. For each layer, the average values of the geotechnical parameters are reported in Table 1.

TLS and Bathymetric Survey

To obtain the 3D digital model of the landslide, a frontal survey from the right riverbank and two lateral surveys from both sides of the landslide (on the intact and still stable road) were executed with a long-range TLS. The lateral observations were necessary to cover even the smallest shadow effects. Then, the frontal position was fixed for the entire time of monitoring to evaluate the residual displacements (Fig. 5). The TLS technique provided high-resolution point clouds that allowed for the reconstruction of the observed targets with a centimeter to millimeter resolution (Jaboyedoff et al. 2012; Fanti et al. 2013). In fact, this technique exploits the time of flight calculation of a laser pulse sent out and back-scattered by different targets to measure distances. The absolute position of each point of the TLS point cloud was defined by coupling the TLS sensors with an inertial system and a GPS (Gigli et al. 2014a). The employed TLS device is a RIEGL LMS-Z420i (Gigli et al. 2014b), and six different complete surveys were performed. In addition, a compact and lightweight laser scanner (FARO, Focus3D CAM2) suitable for interior surveying was further used to precisely triangulate the actual positioning of the culvert (arcuate pattern in Fig. 6) with respect to the displaced material and other anthropic works. In this case, two scan measurements were sufficient to cover the entire studied stretch. One measurement

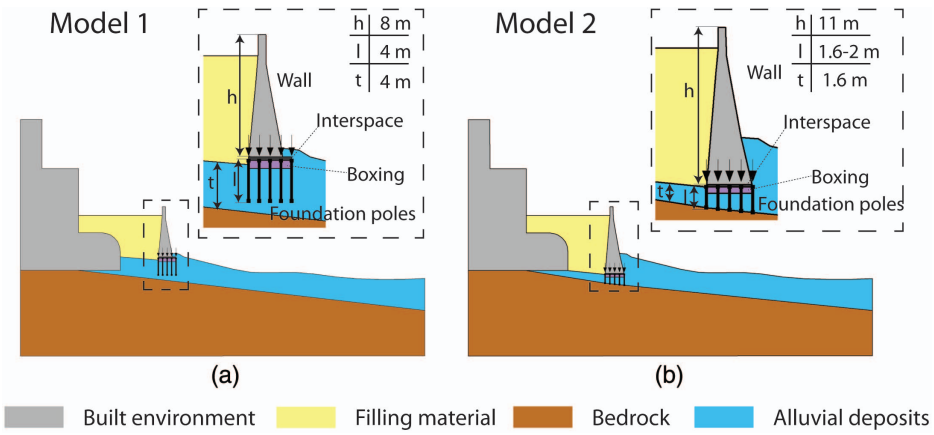

Fig. 6. (Color) (a and b) Two models employed in stability analysis (see text for characteristics); h is wall height, l is wood foundation poles, and t is alluvial deposits' thickness.

was obtained from the outlet, and the other was obtained from a central position, descending from the cellar of an overlying building.

In addition to the previously mentioned surveys, a bathymetric survey of the Arno River portion located in front of the landslide was performed by the Department of Civil and Environmental Engineering of the University of Florence through the application of multibeam sonar techniques. In particular, a multibeam echo sounder was used (1) to map the river floor in front of the landslide to evaluate the presence or the absence of accumulations caused by the landslide; and (2) to evaluate conservation status of the retaining wall's submerged part.

Geophysical Surveys (ERT, DH, and SN)

Geophysical investigations are based on detecting changes in subsurface physical properties (e.g., electrical resistivity, seismic wave velocities, and density), and selecting a more suitable combination of methods is a trade-off between cost to time ratio, advantages (e.g., resolution, diagnostic capability, depth of investigation), and intrinsic limitations and ambiguities of each method (Pazzi et al. 2019). The 3D-ERTs were performed (1) to locate the nineteenth-century culvert, (2) to define the boundary between stable and unstable soil in the embankment, and (3) to characterize the soil on the side of the retaining wall both on the street and on the riverside. The ERTs were collected by means of a Syscal Pro georesistivimeter (IRIS Instruments) coupled with four multichannel cables at 24 channels (i.e., 96 electrodes) with an electrode spacing of 1 m. The dipole-dipole arrays were used to enhance the lateral resolution at shallow depths.

The interface of filling materials and alluvial deposits was determined by means of the downhole, and Poisson's ratio as well as shear, Young's, and bulk moduli were also measured. The shear-wave (SH) and P-wave profiles were acquired by means of triaxial geophones (nominal frequency: 10 Hz). The horizontal to vertical (H/V) single-station seismic noise acquisitions were recorded using five Tromino all-in-one compact three-directional tromograph instruments (MoHo Instruments, Venice, Italy). Each measure ran at 256 Hz for 30 min. The local seismic velocity profiles were reconstructed constraining each trace with soil density and porosity values deduced by laboratory and downhole survey results (Pazzi et al. 2017b). Moreover, the H/V measures aligned in parallel and perpendicular to the embankment wall were interpolated to generate synthetic contour maps of H/V.

Riverbank Stability Analysis

The riverbank stability analysis of the Lungarno Torrigiani sector affected by the landslide of May 25, 2016, was carried out using the limit equilibrium method outlined by Morgenstern and Price (1965). Since the visual inspection carried out after the field excavation has revealed sheared wood foundation piles, the shear has been assumed as the main failure mechanism. The Slope/W–Geostudio 2012 software was used for the analysis (Agostini et al. 2014; Fidolini et al. 2015; Nocentini et al. 2015). The stability conditions were verified considering a section perpendicular to the Lungarno Torrigiani passing through the center of the cusp. The topographic section used in the analysis was reconstructed on the basis of the TLS and bathymetric surveys. The lithological and geotechnical characteristics of the material were derived from the interpretation of the boreholes and the geotechnical characterization (section "Boreholes and Geotechnical Characterization," Table 1), while the reconstruction of the depth and type of the foundation of the retaining wall was reconstructed from boreholes and geophysical surveys as well as from the original design models made by the architect and engineer Poggi (1882) for the urban renovation.

In relation to the variability of the data resulting from the surveys performed and the uncertainty on the depth of the base of the wall, two different models were proposed (Model 1 and Model 2 in Fig. 6). The models, which were realized by taking into account sections normal to the wall, differ from each other regarding wall height (h in Fig. 6), the length of the wood foundations piles (l in Fig. 6), and the thickness of alluvial deposits (t in Fig. 6).

The construction technique of the wall did not use the poles as foundation but as reinforcement material to stabilize the foundation substrata. Therefore, the wall foundation needs to be considered as a direct foundation on a reinforced substratum with the piles. Because of these construction features, a thin virtual interspace material at the wall base was introduced in the model. In addition, referring to the wall historical projects, another level of material, boxing, consists of rock blocks and gravel and was introduced in the models. The geotechnical parameters for both interspace and boxing are reported in Table 1.

Based on the analysis of the Poggi's project (1882), four piles were considered for the stability analysis along the considered section. The piles are made of pinewood and have a diameter of approximately 20 cm. The shear force of the single pile has been considered in the analysis and was evaluated based on the shear strength of pinewood and the pile diameter. The shear strength of the pinewood piles has been defined as 6 MPa, based on literature values directly derived for the SLOPE/W library.

A steady-state stability analysis was carried out considering different water levels in the filling material. In particular, the slope stability analysis was performed by considering the following for Model 1: (1) dry conditions; (2) water table equal to Arno River low-level discharge; (3) water table equal to Arno River high-level discharge; (4) complete saturation of filling material due to pipe rupture and low river level; (5) saturation of filling material until limit equilibrium conditions and low river level. For Model 2, only conditions (1), (2), (3), and (4) were examined. Slope stability analyses were conducted in terms of effective stress using the Mohr-Coulomb criterion. For both models and for each saturation configuration, the critical sliding surface with the lower factor of safety (FS) was determined.

Characterization of the Retaining Wall Crack Pattern

The structural deterioration/damage level is defined as *health* in civil engineering; damages and aging monitoring and detection play a central role in protection, restoration, and consolidation of cultural heritage sites (Chang et al. 2003). Moreover, nondestructive methods must be employed due to historical structures preservation needs (Chang et al. 2003; Lubowiecka et al. 2009; Tarchi et al. 2010; Aguilar et al. 2015). Therefore, the following techniques were employed to monitor the crack pattern of the Lungarno Torrigiani masonry embankment wall: digital photogrammetry (DP), TLS, ERT, and SN measures.

Photogrammetric and TLS Survey

A DP survey was performed to provide a 3D reconstruction of the crack patterns on the damaged part of the wall. DP is currently a commonly used technique for the reconstruction of 3D surface models starting from a set of optical images. This process can be performed using one of several Structure-from-Motion (SfM) software programs that exploit specific algorithms for image triangulation and bundle adjustment for the reconstruction of very accurate 3D representations of any object or surface (Westoby et al. 2012). The result of digital photogrammetric processing is a point cloud that is obtained by triangulating the position in the 3D space of pixels that are visible in two or more images with a good overlap (generally >60%).

In this work, the DP survey was performed using 33 high-resolution images acquired manually from a small boat moving parallel to the riverbank. The photos were taken using a Sony Alpha 7R2 camera with a 35-mm full-frame CMOS sensor, 42.4-MPix resolution (image size 7,952 × 5,304 pixels), and an estimated overlap of approximately 80% at an average distance of 20 m from the embankment. Photos were processed using Agisoft Photoscan Professional software (Agisoft 2016). The resulting high-resolution color point cloud was integrated with acquired data using TLS to characterize the cracks pattern on the damaged part of the wall in three dimensions. This process was possible due to the very high point density of the resulting red, green, blue (RGB) point cloud with an average value of 59,000 points per square meter on the whole damaged part of the wall.

The photogrammetric point cloud was extremely useful since it provided a more detailed cloud with respect to the TLS due to the distance between the TLS position and the wall, which did not allow the acquisition of a sufficiently dense RGB point cloud for use to precisely draw the cracks. On the other hand, TLS and photogrammetric clouds were very usefully integrated to obtain the coordinates of visible objects in the TLS cloud to be used as ground control points (GCPs) for photogrammetric processing. This feature was very important because the area on the top of the wall and on the buildings behind were completely inaccessible, making it impossible to measure manually the coordinates of points and objects in the scene using a RTK-GPS technique (Tapete et al. 2015). A total of 11 GCPs were chosen for photogrammetric processing based on objects that can be easily recognized in the TLS cloud with a homogeneous spatial distribution in the observed scene. The resulting average error calculated for the whole GCPs data set is 0.075 m in XYZ direction, and a comparison between the photogrammetric and the laser scanner cloud performed using the CloudCompare software (Girardeau-Montaut 2015) yielded average distances within 5–7 cm.

ERT Survey

The 3D-ERTs were performed to characterize the basement of the wall and to evaluate its continuity after the riverbank landslide. The electrodes were spaced 1 m apart and placed at the foot of the embankment wall simultaneously in the hole generated by the landslide and on the riverbank. Dipole-dipole arrays were used.

Wall Seismic Vibrations Survey

As reported in the literature, vibration-based methodologies are widely used both to characterize the soil frequency (Lermo and Chavez-Garcia 1993; Larose et al. 2015; Lotti et al. 2015; Pazzi 2017b, 2017c; Del Soldato et al. 2018) and to provide useful information on the structure's conditions and damages (Spizzichino et al. 2013; Asteris et al. 2014; Ceravolo et al. 2014; Pazzi et al. 2016a, b). The national and international regulations define the maximum values of seismic velocities acceptable for a historical structure, such as the Lungarno Torrigiani masonry embankment wall, and specify that the spectral analysis allows one to identify the frequencies and amplitudes of the vibration harmonic components. Moreover, it is well known that worksite activities are run using high-energy content and frequencies that could damage historical structures/buildings.

Pazzi et al. (2017a) described the SN array employed to monitor the seismic response of the Lungarno Torrigiani masonry embankment wall during the conservation works. The seismic network was drawn up (1) to define the wall resonance frequencies after the landslide induced damages, (2) to quantify the vibrations induced by the conservation/consolidation activities, (3) to assess the double resonance phenomena, (4) to verify the compatibility with the standards, and (5) to measure any critical conditions during the conservation works. The fundamental frequency of the masonry embankment wall was evaluated by means of the horizontal-to-vertical spectral ratio technique (Nakamura 1989; Del Gaudio et al. 2014; Pazzi et al. 2017c), which was between 4 and 15 Hz and consistent with the frequency range of an approximately 10-meter high, squat, and monolithic structure (Pazzi et al. 2017a).

The SN array consists of three high-gain triaxial velocimeters located in the three structurally more fragile and fractured areas: LGT101 near the hinge on the side of Ponte alle Grazie, LGT102 near the cusp, and LGT103 near the hinge on the side of Ponte Vecchio (Fig. 5). The vibration monitoring ran at 200 Hz from August 14 to October 10, 2016, and the whole period can be divided into three intervals according to the different kinds of works: (1) piling work; (2) parapet breakdown, excavation, embankment arrangement, and Arno River side foot wall consolidation; and (3) backfill and restoration of the original condition via standard construction activities.

Results

Failure Characterization

The laboratory tests on samples allow recognizing three different material typologies from top to bottom: filling material, alluvial deposits, and claystone substrata (top of Sillano Formation) (Table 1). The filling material and the alluvial deposits were classified (ASTM 1985) as silty sand (SM), while the Sillano Formation is classified as low plasticity silt (ML). In general, all the soils exhibit a low plasticity behavior with a plasticity index (Ip) ranging from 5 to 9. The shear strength parameters of filling material and alluvial deposits are typical of granular soils with cohesion equal to zero kPa and average frictional angles (°) of 26° and 35°, respectively. Sillano substrata have an average frictional angle (°) of 26° and cohesion of 10 kPa. Geotechnical parameters derived from the downhole survey are also summarized in Table 1.

The TLS analyses allowed the exact landslide geometry to be characterized and the involved volumes to be defined. The cavity generated by the street collapsing is approximately 1,303 m^3, while the wall deformation toward the Arno River is approximately 1,180 m^3. The ERT results clearly show that the soil on the side of the retaining wall both on the street and on the riverside has resistivity values of approximately 50–60 Ωm [Fig. 7(a)]. Nevertheless, it was not possible to differentiate the discontinuity between the filling material and the alluvial deposits because they have similar resistivity ranges according to the resistivity ranges available in the literature (Raynolds 2011). The Poggi's culvert location is clearly identified by both the ERT (resistivity values greater than 200 Ωm) and H/V surveys (Fig. 7). The H/V curves and consequently the contour maps [Fig. 7(b)] clearly show velocity inversion [blue areas in Fig. 7(b)] at low depths (Castellaro and Mulargia 2009) associated with an underground tunnel.

Riverbank Stability Analysis

The riverbank stability analysis results are presented in Fig. 8. Five saturation configurations are tested for Model 1, while four configurations are tested for Model 2. For both models and each configuration, the sliding surface with the lower factor of safety is reported in Fig. 8. In Model 1, the lower FS is noted in condition of complete saturation of the filling material and low river level discharge with a Safety Factor (FS) equal to 0.7. For Model 1, the instability condition (FS =1) was also verified for the case of partially saturated filling. For Model 2, the limit equilibrium condition (FS = 1.0) was verified in the condition of completely

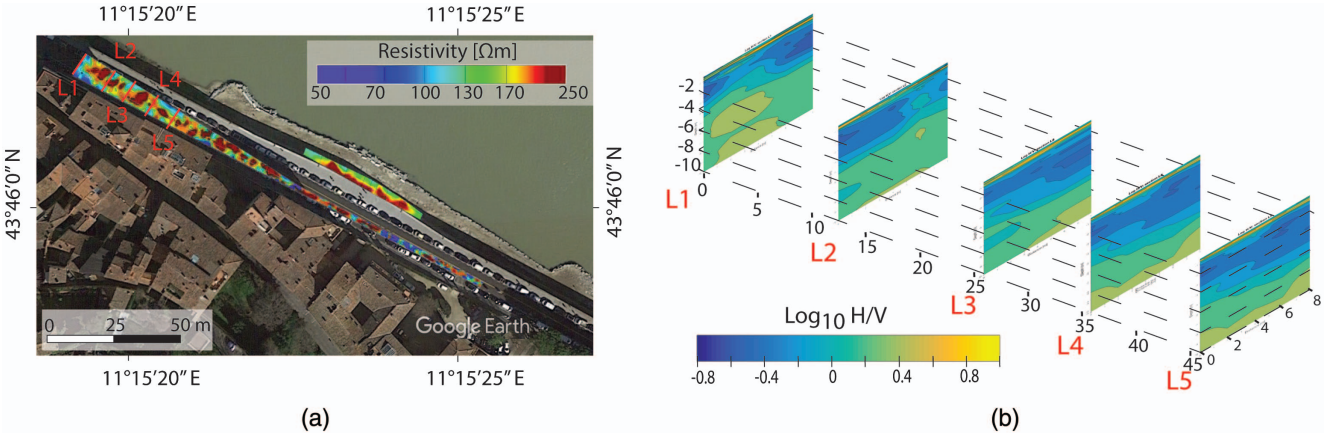

Fig. 7. (Color) (a) 2D horizontal view of ERT survey carried out on street and riverside of wall during October 3, 2017, satellite image (map data © 2020 Google); and (b) H/V contour maps perpendicular to embankment wall.

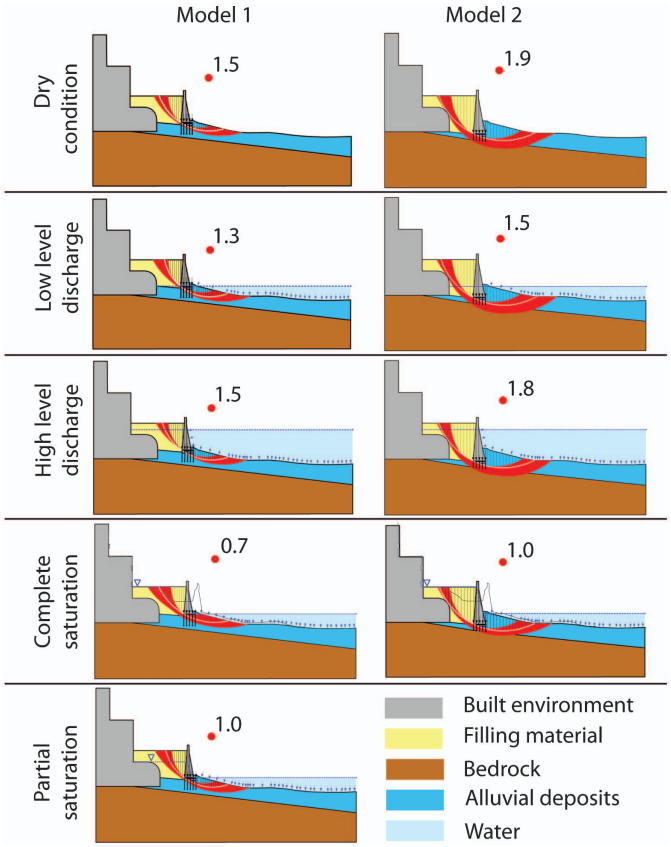

Fig. 8. (Color) Stability analysis results with Model 1 on left column and Model 2 on right column; critical slope surface is presented in white, while dots with numbers indicate related minimum factor of safety value. In results of two models, under complete saturation condition, post failure profile is reported in gray. Models 1 and 2 differ with regard to wall height, length of wood foundation poles, and thickness of alluvial deposits (for details see Fig. 6). For each model, five different saturation conditions have been taken into account: (1) dry conditions; (2) water table equal to Arno River low level discharge; (3) water table equal to Arno River high level discharge; (4) complete saturation of filling material due to pipe rupture and low river level; and (5) saturation of filling material until limit equilibrium conditions and low river level.

saturated filling material and low river level discharge. The critical failure surfaces identified by the model have a circular shape, crossing the filling material and the alluvial deposits.

Embankment Wall Characterization

The DP cloud results allowed precise mapping of three fracture systems on the wall, corresponding to the Ponte Vecchio side hinge, the Ponte alle Grazie side hinge, and the central cusp (Fig. 9). In the two side sectors, the fracture systems are characterized by main cracks with an average width of 5–8 cm along with some minor fractures caused by the intense deformation of the part. The cusp zone is characterized by a more complex fissure pattern with a main fracture that ramifies in the lower part and a set of nine subparallel cracks spaced 4–5 m from each other with maximum visible length of 2 m. No fractures were detected in the parts between the lateral hinges and the cusp with the exception of a longitudinal crack mapped on the upper part of the wall between the Ponte alle Grazie side hinge and the cusp. Moreover, the bathymetric survey showed that the submerged part of the wall was deformed without collapsing.

The high resistivity anomalies (values greater than 200 Ωm and warm colors) up to a depth of 3 m shown in Fig. 10 and characterized by an elongated shape are associated with the foundations of the embankment wall. The results [in particular the vertical section C in Fig. 10(c)] also show that the riverbank landslide deformed these foundations since the high resistivity anomaly is not continuous. Moreover, the high resistivity values indicate that the basement moved toward the Arno River more than the embankment wall, and a partial basement collapse occurred at a depth of approximately 3 m. The trend of the peak component particle velocity (i.e., the maximum value of one of the velocity vectors for three components, measured at the same time at a given point, Fig. 11) clearly shows the work advancement. The signal spectra analysis (Fig. 11) indicates that, until the end of the piling work, the most stressed component is the one perpendicular to the wall, and the higher energy content is between the frequency of 10 and 20 Hz (Pazzi et al. 2017a). Finally, as shown in Pazzi et al. (2017a), the SN monitoring revealed that the hinge zones seem to be similar to high-pass filters and therefore more easily affected by low-frequency content vibrations (i.e., the August 24, 2016, earthquake), while the cusp section is more affected by high-frequency content (i.e., on site conservation works).

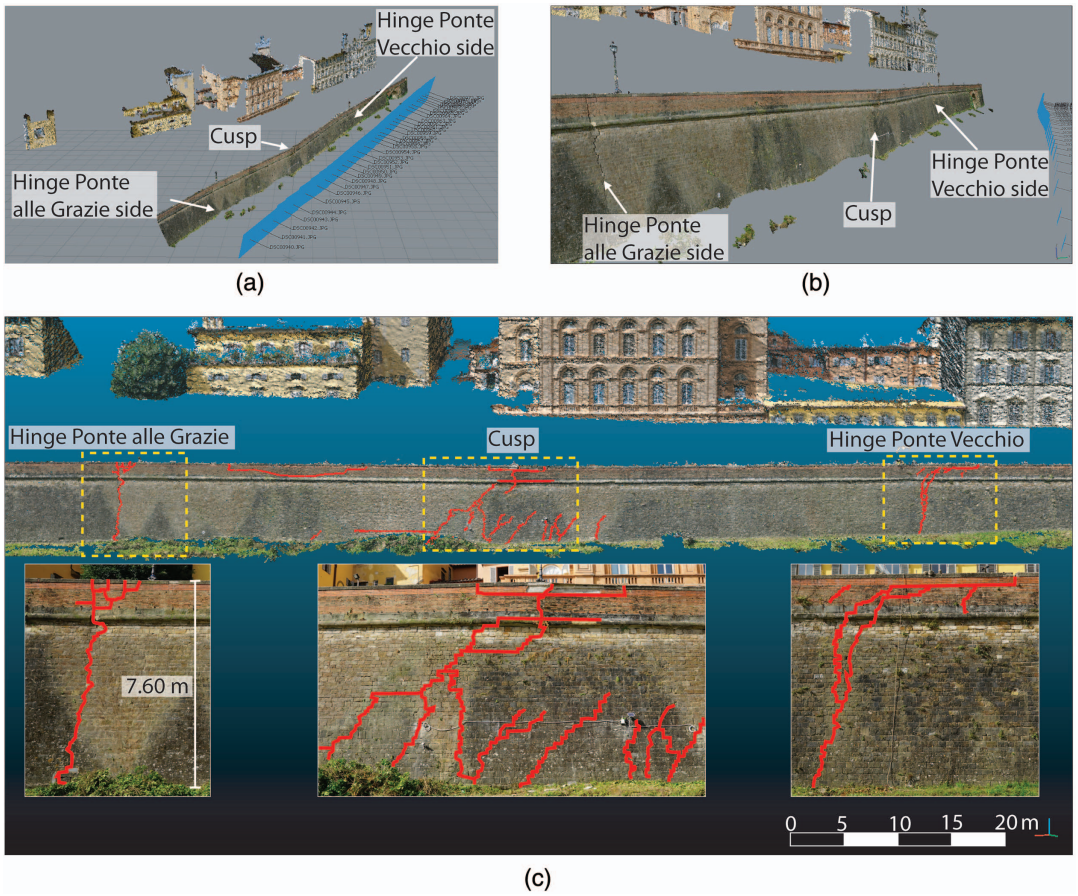

Fig. 9. (Color) Results of photogrammetric processing: (a and b) two views of a point cloud in Agisoft Photoscan Professional showing position of cameras; and (c) overall view of mapped fracture systems on wall. (Images by L. Tanteri.)

Discussion

The evolution of the studied collapse is the result of the combination and interaction of two different dynamics. The first feature is the riverbank failure, a typical destructive phenomenon during extreme hydraulic conditions, such as the highly concentrated water circulation on the slope behind the riverbank or high-water levels in the riverbed after exceptional rainfalls. These critical conditions, which are occasionally intensified and worsened by landslides and debris floods, are well known throughout the history of the city, especially after the intense urbanization starting from 1,175 (see section "The Instabilities of Previous Riverbanks," [Fig. 3). The second factor is the continuous loss of water from the subterranean pipes of the aqueduct, which is a more recent phenomenon that developed from the capillary diffusion of the modern structure in every part of the city (completed with the nineteenth-century works). In recent decades, this dense network has undergone minimal maintenance and has suffered sudden localized breakages and abundant leakages with repercussions on daily city life. In some circumstances, the safety and health of most of the citizens have been put at risk (Morelli et al. 2014). When these second events occurred along artificial embankments or riverbanks, they could contribute to the stability reduction even in the absence of traditional causes due to meteorological events. Moreover, they might have influenced the way in which the landslide moved and developed.

From our investigations, we can deduce that a significant breakage of the aqueduct located along the riverbank first occurred, and an abundant flow of water was dispersed in the surrounding soil until its complete saturation. Then, water reached the road level, and the embankment collapsed only a few hours after the structural damage at the main pipe. This event was demonstrated by the stability analysis that confirms the failure occurred upon the complete saturation of the embankment and at low river levels. Nonetheless, despite the fragility of the most modern infrastructures of the aqueduct, the culvert and the retaining wall of the riverbank contained the part of the landslide that remained spatially confined. Investigations performed using TLS, DP, and ERT show that both the aerial and submerged parts of the wall were deformed without collapsing, while SN monitoring, which was performed during the restoration works, showed that the most stressed component is that perpendicular to the wall. The wall structure of the culvert, which is transverse to the movement, seems to have stopped the retrogression toward the buildings without causing deformations. In contrast, the external retaining wall with a parallel pattern slid only for a few meters toward the watercourse, fracturing only along points at higher tension (viz., at the edges of the landslide and in the central portion). During the material translation, which occurred in a single moment, the entire wall did not shatter or topple, demonstrating the good execution of the nineteenth-century works from the foundations to the main body. During this episode, only a minimal amount of material was deposited in the Arno riverbed following the local current.

Then, thanks to rapid interventions based on the deployment of several technical means and experiences in the field of cultural heritage and human life preservation, sufficient interdisciplinary forces

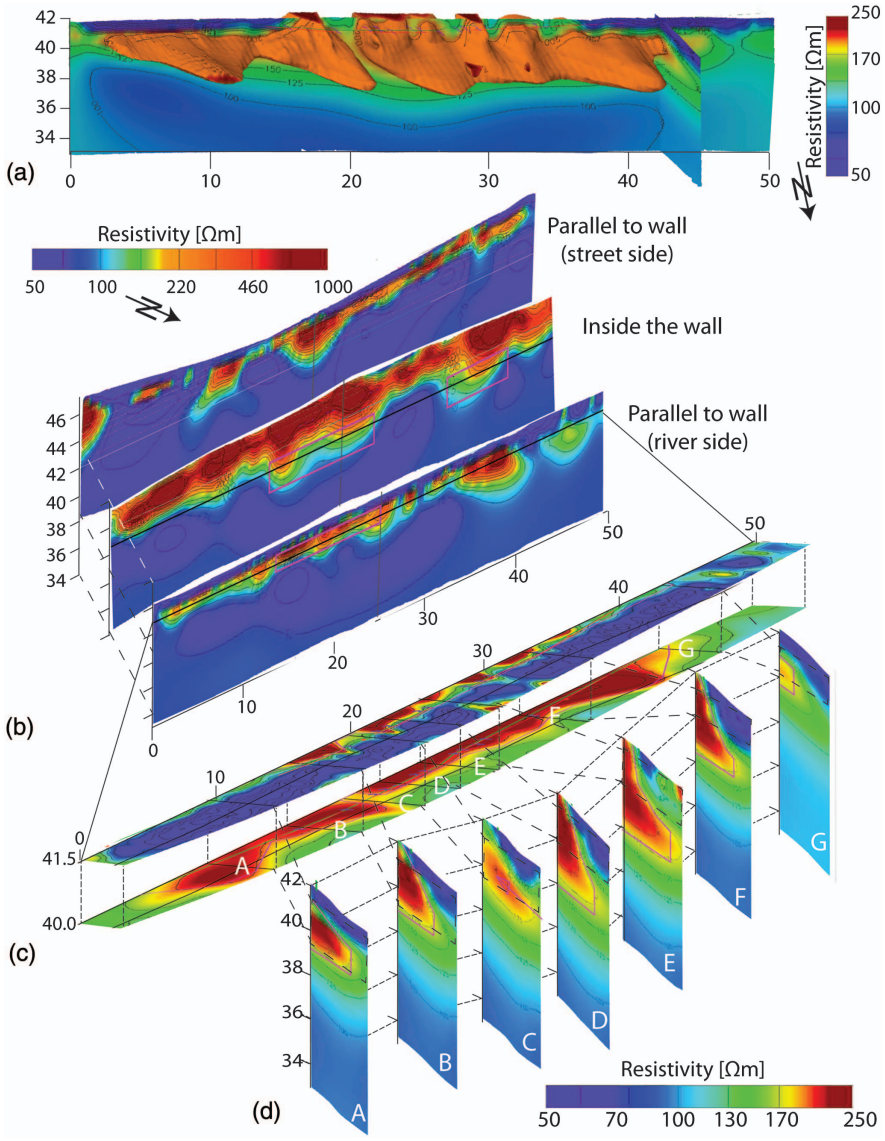

Fig. 10. (Color) (a) 3D view from Arno River of deformed embankment wall; (b) 2D vertical slices parallel to wall on street side, inside wall and parallel to wall on riverside; (c) 2D horizontal slices of first 1.5 m; and (d) 2D vertical slices perpendicular to wall (riverside point of view).

for the management of the emergency and the return to normality were put in place, avoiding further negative damage or additional criticality for the population. At the end, the wall, which remained fixed in the same position for the whole time of works, was preserved with this new geometry since the residual conditions of the structure were suitable for this operation. According to the technicians, the hydraulic section decrease does not seem to be significantly compromised in relation to the urban flood risk.

Conclusions

Many Italian cultural heritage sites frequently suffer multiple hazards. Only through a synergistic coordination of interventions and available economic resources, a real policy for their protection and conservation can be effectively sustained. This paper presents the results of an integrated study performed to characterize a riverbank landslide that affected the UNESCO site of Florence. On May 25, 2016, a portion of the artificially built riverbank collapsed just a few meters away from the famous Ponte Vecchio bridge, endangering the stability of a wider portion of the historic heritage site. To identify the condition of damage of the involved structures, to define the causes of the failure, and to mitigate and preserve the cultural heritage site, a detailed analysis of this event was performed based on the integration of boreholes and geotechnical characterization, remote-sensing techniques, stability analyses, and geophysical surveys.

Three different material typologies were identified from top to bottom, through boreholes: filling material, alluvial deposits, and claystone substrata (top of Sillano Formation). TLS survey results have been used to characterize the exact landslide geometry and to estimate the involved volumes. The cavity generated by the street collapse was approximately 1,303 m^3, while the volume of the displaced mass toward the Arno River was approximately 1,180 m^3. The riverbank stability analysis result demonstrates that a lower safety factor was obtained when the filling material was completely saturated, and the river level was low. Thus, the major cause of the collapse can be attributed to the loss of water from the local subterranean pipes. The TLS, DP, and ERT surveys were performed to characterize the embankment wall damage and identified a

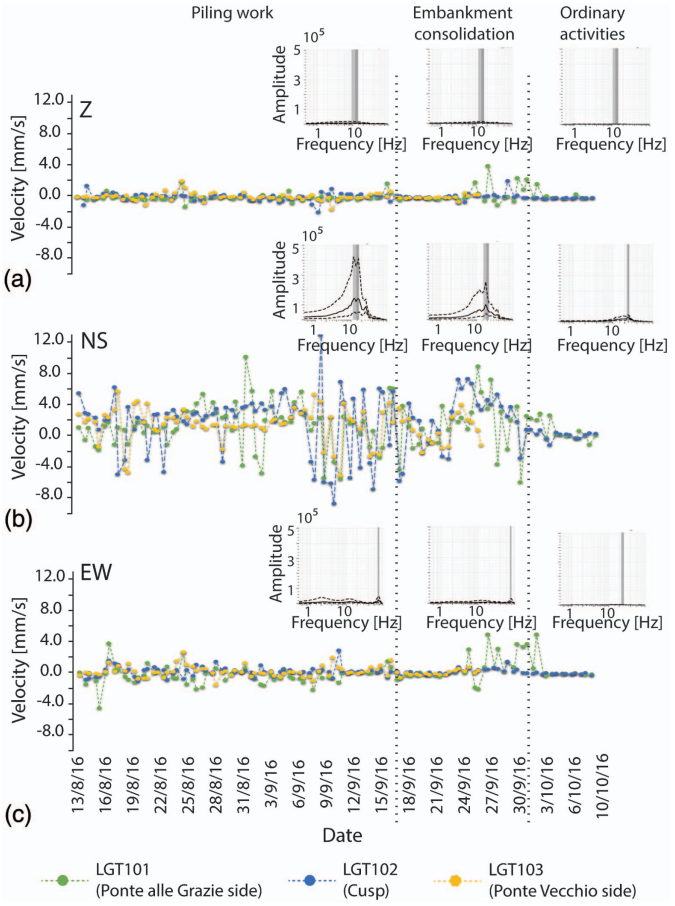

Fig. 11. (Color) Peak component particle velocity every 12 h and signal spectral analysis of three components: (a) Z; (b) NS; and (c) EW of each station (LGT101: green, LGT102 blue, and LGT103 yellow). Black dotted lines separate three time intervals corresponding to three different types of work: piling work, embankment consolidation, and ordinary activities. (Adapted from Pazzi et al. 2017a.)

complex pattern of deformations, which did not cause the wall collapse.

The traditional and modern techniques used here were inexpensive and could be successfully employed to reduce the disaster risk at cultural heritage sites at risk of geohydrological hazards. The employed techniques provide information that is useful for planning emergency interventions and for supporting the following restoration activities.

Data Availability Statement

Some or all data, models, or code generated or used during the study are available from the corresponding author by request (boreholes stratigraphy and geotechnical data, terrestrial laser scanner data, bathymetric data, geophysical surveys data).

Acknowledgments

This work was carried out in the framework of Florence mayor ordinance No. 2016/00133 of May 27, 2016, and subsequent modifications and integrations. We would like to thank SOING Strutture e Ambiente s.r.l. for helping perform the geophysical surveys. We also would like to thank all the people in charge of the GB-InSAR monitoring and Emanuele Intrieri and Laura Pastonchi for their help in collecting historical and geological materials.

References

Abbate, E., and M. Sagri. 1970. "The Eugeosynclinal sequences." *Sediment. Geol.* 4 (3–4): 251–340. https://doi.org/10.1016/0037-0738(70)90018-7.

Agisoft, L. L. C. 2016. "Agisoft PhotoScan Professional v. 1.2.4." Accessed March 26, 2018. http://www.agisoft.com.

Agostini, A., V. Tofani, T. Nolesini, G. Gigli, L. Tanteri, A. Rosi, S. Cardellini, and N. Casagli. 2014. "A new appraisal of the Ancona landslide based on geotechnical investigations and stability modelling." *Q. J. Eng. Geol. Hydroge.* 47 (1): 29–43.

Aguilar, R., R. Marques, K. Sovero, C. Martel, F. Trujillano, and R. Boroschek. 2015. "Investigations on the structural behaviour of archaeological heritage in Peru: From survey to seismic assessment." *Eng. Struct.* 95 (Jul): 94–111. https://doi.org/10.1016/j.engstruct.2015.03.058.

Asteris, P. G., M. P. Chronopoulos, C. Z. Chrysostomou, H. Varum, V. Plevris, N. Kyriakides, and V. Silva. 2014. "Seismic vulnerability assessment of historical masonry structural systems." *Eng. Struct.* 62–63 (Mar): 118–134. https://doi.org/10.1016/j.engstruct.2014.01.031.

ASTM. 1985. *Classification of soils for engineering purposes: Annual Book of ASTM Standards*. ASTM D2487-83. West Conshohocken, PA: ASTM.

ASTM. 1998. *Standard practice for wet preparation of soil samples for particle-size analysis and determination of soil constants*. ASTM D2217–85. West Conshohocken, PA: ASTM.

ASTM. 2007. *Standard test method for particle-size analysis of soils*. ASTM D422–63. West Conshohocken, PA: ASTM.

ASTM. 2010. *Standard test methods for liquid limit, plastic limit, and plasticity index of soils*. ASTM D4318–10. West Conshohocken, PA: ASTM.

Bicocchi, G., V. Tofani, M. D'Ambrosio, C. Tacconi-Stefanelli, P. Vannocci, N. Casagli, G. Lavorini, M. Trevisani, and F. Catani. 2019. "Geotechnical and hydrological characterization of hillslope deposits for regional landslide prediction modeling." *B. Eng. Geol. Environ.* 78 (7): 4875–4891. https://doi.org/10.1007/s10064-018-01449-z.

Boccaletti, M., et al. 1997. "Geologia urbana di Firenze. In: Geologia delle grandi aree urbane—Progetto Strategico CNR [Urban Geology of Florence. In: Geology of big urban area—CNR strategic plan]." In *Proc., Compositori*, 49–93. Rome: Consiglio Nazionale delle Ricerche.

Boccaletti, M., and M. Coli, cartographers. 1982. *Carta strutturale dell'Appennino settentrionale, 1: 250.000 scale map. CNR Progetto Finalizzato Geodinamica.* Publication n. 429. Florence, Italy: Società Elaborazioni Cartografiche.

Briganti, R., G. Ciufegni, M. Coli, and S. Polimeni, and G. Pranzini. 2003. "Underground florence: Plio-quaternary geological evolution of the Florence area." *Boll. Soc. Geol. Ital.* 122 (3): 435–445.

Canfarini, A. 1978. "Il deflusso delle piene dell'Arno in Firenze. Il ribassamento delle platee dei ponti Vecchio e a Santa Trinita." [The outflow of the Arno high water levels in Florence. The lowering of the foundation mat of Ponte Vecchio and Santa Trinita bridges]." *Bollettino degli Ingegneri* 1978 (8–9): 2–17.

Canuti, P., C. Cencetti, M. Rinaldi, and P. Tacconi. 1994. "The fluvial dynamics of the Arno River: 2. Historical evolution of the Arno river bed." In Vol. of 48 *Proc. of the 76th Summer Meeting of the Società Geologica Italiana Part 3, Memorie della Società Geologica Italiana*, edited by S. Moretti, 851–864. Roma: Società Geologica Italiana.

Canuti, P., C. Margottini, R. Fanti, and E. N. Bromhead. 2009. "Cultural heritage and landslides: Research for risk prevention and conservation." In *Landslides—Disaster risk reduction*, edited by K. Sassa, and P. Canuti. Berlin: Springer.

Capecchi, F., G. Guazzone, and G. Pranzini. 1975. "Il bacino lacustre di Firenze-Prato-Pistoia. Geologia del sottosuolo e ricostruzione evolutiva." [The lake basin of Florence-Prato-Pistoia. Subsoil geology and evolutionary reconstruction]." *Boll. Soc. Geol. It.* 94: 637–660.

Casagli, N., W. Frodella, S. Morelli, V. Tofani, A. Ciampalini, E. Intrieri, F. Raspini, G. Rossi, L. Tanteri, and P. Lu. 2017a. "Spaceborne, UAV and ground-based remote sensing techniques for landslide mapping, monitoring and early warning." *Geoenviron. Disasters* 4 (1): 9. https://doi.org/10.1186/s40677-017-0073-1.

Casagli, N., S. Morelli, W. Frodella, E. Intrieri, and V. Tofani. 2018. "TXT-tool 2.039-3.2 ground-based remote sensing techniques for landslides mapping, monitoring and early warning." In *Landslide dynamics: ISDR-ICL landslide interactive teaching tools*, edited by K. Sassa, F. Guzzetti, H. Yamagishi, Ž. Arbanas, N. Casagli, M. McSaveney, and K. Dang, 255–274. Cham, Switzerland: Springer.

Casagli, N., V. Tofani, S. Morelli, W. Frodella, A. Ciampalini, F. Raspini, and E. Intrieri. 2017b. "Remote sensing techniques in landslide mapping and monitoring, keynote lecture." In *Advancing culture of living with landslides. Volume 3: Advances in landslide technology*, edited by M. Mikos, Ž. Arbanas, Y. Yin, and K. Sassa, 1–19. Cham, Switzerland: Springer.

Castellaro, S., and F. Mulargia. 2009. "The effect of velocity inversions on H/V." *Pure Appl. Geophys.* 166 (4): 567–592. https://doi.org/10.1007/s00024-009-0474-5.

Catenacci, V. 1992. *Il dissesto geologico e geoambientale in Italia dal dopoguerra al 1990. [Geological and geo-environmental disruption in Italy from the post-war period to 1990]*. Rome: Istituto Poligrafico e Zecca dello Stato.

Cencetti, C., and P. Tacconi. 2005. "The fluvial dynamics of the Arno River." *Giornale di Geologia Applicata* 1: 193–202.

Ceravolo, R., G. Pistone, L. Zanotti Fragonara, S. Massetto, and G. Abbiati. 2014. "Vibration-based monitoring and diagnosis of cultural heritage: A methodological discussion in three examples." *Int. J. Archit. Herit.* 10 (4): 375–395. https://doi.org/10.1080/15583058.2013.850554.

Chang, P. C., A. Flatau, and S. C. Liu. 2003. "Review paper: Health monitoring of civil infrastructure." *Struct. Health Monit.* 2 (3): 257–267. https://doi.org/10.1177/1475921703036169.

Chen, F., J. You, P. Tang, W. Zhou, N. Masini, and R. Lasaponara. 2018. "Unique performance of spaceborne SAR remote sensing in cultural heritage applications: Overviews and perspectives." *Archaeol. Prospect.* 25 (1): 71–79. https://doi.org/10.1002/arp.1591.

Coli, M., and P. Rubellini. 2007. *Note di Geologia Fiorentina. [Florentine Geology Notes]*. Florence, Italy: Società Elaborazioni Cartografiche.

De Finis, E., P. Gattinoni, and L. Scesi. 2017. "Hydrogeological hazard in the Unesco world heritage site of Castelseprio (northern Italy)." *Int. J. Heritage Archit.* 1 (2): 256–266. https://doi.org/10.2495/HA-V1-N2-256-266.

Del Gaudio, V., S. Muscillo, and J. Wasowski. 2014. "What we can learn about slope response to earthquakes from ambient noise analysis: An overview." *Eng. Geol.* 182 (Part B): 182–200. https://doi.org/10.1016/j.enggeo.2014.05.010.

Del Soldato, M., V. Pazzi, S. Segoni, P. De Vita, V. Tofani, and S. Moretti. 2018. "Spatial modeling of pyroclastic cover deposit thickness (depth to bedrock) in peri-volcanic areas of Campania (southern Italy)." *Earth. Surf. Proc. Land.* 43 (9): 1757–1767. https://doi.org/10.1002/esp.4350.

De Zolt, S., P. Lionello, A. Nuhu, and A. Tomasin. 2006. "The disastrous storm of 4 November 1966 on Italy." *Nat. Hazard Earth. Sys.* 6 (5): 861–879. https://doi.org/10.5194/nhess-6-861-2006.

Fanti, R. 2006. "Slope instability of San Miniato hill (Florence, Italy): Possible deformation patterns." *Landslides* 3 (4): 323–330. https://doi.org/10.1007/s10346-006-0060-1.

Fanti, R., G. Gigli, L. Lombardi, D. Tapete, and P. Canuti. 2013. "Terrestrial laser scanning for rockfall stability analysis in the cultural heritage site of Pitigliano (Italy)." *Landslides* 10 (4): 409–420. https://doi.org/10.1007/s10346-012-0329-5.

Fidolini, F., V. Pazzi, W. Frodella, S. Morelli, and R. Fanti. 2015. "Geomorphological characterization, monitoring and modeling of the Monte Rotolon complex landslide (Recoaro Terme, Italy)." In *Engineering geology for society and territory. Volume 2: Landslide processes*, edited by G. Lollino, D. Giordan, G. B. Crosta, J., Corominas, R., Azzam, J., Wasowski, and N. Sciarra, 1311–1315. Cham, Switzerland: Springer.

Frati, M. 2015. "Questo diluvio fece alla città e contado di Firenze infinito danno". Danni, cause e rimedi nell'alluvione del 1333. ["This deluge did infinite damage to the city and countryside of Florence". Damages, causes and remedies in the 1333 flood]." *Città e Storia* 10 (1): 41–60.

Geoscopio. 2013. "Geographical database of Tuscany region." Accessed June 17, 2018. https://www.regione.toscana.it/-/geoscopio.

Gigli, G., W. Frodella, F. Garfagnoli, F. Mugnai, S. Morelli, F. Menna, and N. Casagli. 2014a. "3-D geomechanical rock mass characterization for the evaluation of rockslide susceptibility scenarios." *Landslides* 11 (1): 131–140. https://doi.org/10.1007/s10346-013-0424-2.

Gigli, G., W. Frodella, F. Mugnai, D. Tapete, F. Cigna, R. Fanti, E. Intrieri, and L. Lombardi. 2012. "Instability mechanisms affecting cultural heritage sites in the Maltese Archipelago." *Nat. Hazard Earth Sys.* 12 (6): 1883–1903. https://doi.org/10.5194/nhess-12-1883-2012.

Gigli, G., S. Morelli, S. Fornera, and N. Casagli. 2014b. "Terrestrial laser scanner and geomechanical surveys for the rapid evaluation of rockfall susceptibility scenarios." *Landslides* 11 (1): 1–14. https://doi.org/10.1007/s10346-012-0374-0.

Girardeau-Montaut, D. 2015. "Cloud compare: 3D point cloud and mesh processing software." Accessed February 10, 2020. http://www.danielgm.net/cc/.

Guidoboni, E., and G. Ferrari. 1995. "Historical cities and earthquakes: Florence during the last nine centuries and evaluations of seismic hazard." *Ann. Geophys.* 38 (5–6): 617–647.

Jaboyedoff, M., T. Oppikofer, A. Abellán, M. H. Derron, A. Loye, R. Metzger, and A. Pedrazzini. 2012. "Use of LIDAR in landslide investigations: A review." *Nat. Hazards* 61 (1): 5–28. https://doi.org/10.1007/s11069-010-9634-2.

Larose, E. S., et al. 2015. "Environmental seismology: What can we learn on earth surface processes with ambient noise?" *J. Appl. Geophys.* 116 (May): 62–74. https://doi.org/10.1016/j.jappgeo.2015.02.001.

Lermo, J., and F. J. Chavez-Garcia. 1993. "Site effect evaluation using spectral ratios with only one station." *B. Seismol. Soc. Am.* 83 (5): 1574–1594.

Lotti, A., G. Saccorotti, A. Fiaschi, L. Matassoni, G. Gigli, V. Pazzi, and N. Casagli. 2015. "Seismic monitoring of rockslide: The Torgiovannetto quarry (Central Apennines, Italy)." In *Engineering geology for society and territory. Volume 2: Landslide processes*, edited by G. Themistocleous, D. Giordan, G. B. Crosta, J., Corominas, R., Azzam, and J. Wasowski, and N. Sciarra, 1537–1540. Cham, Switzerland: Springer.

Lubowiecka, I., J. Armesto, P. Arias, and H. Lorenzo. 2009. "Historic bridge modelling using laser scanning, ground penetrating radar and finite element methods in the context of structural dynamics." *Eng. Struct.* 31 (11): 2667–2676. https://doi.org/10.1016/j.engstruct.2009.06.018.

Margottini, C., and D. Spizzichino. 2014. "The management of cultural heritage in sites prone to natural hazard." *Mem. Descr. Carta Geol. d'It.* 96: 415–430.

Morelli, S., A. Battistini, and F. Catani. 2014. "Rapid assessment of flood susceptibility in urbanized rivers using digital terrain data: Application to the Arno river case study (Firenze, northern Italy)." *Appl. Geogr.* 54 (Oct): 35–53. https://doi.org/10.1016/j.apgeog.2014.06.032.

Morelli, S., V. H. Garduño-Monroy, G. Gigli, G. Falorni, E. Arreygue Rocha, and N. Casagli. 2010. "The Tancitaro Debris Avalanche: Characterization, propagation and modeling." *J. Volcanol. Geoth. Res.* 193 (1–2): 93–105. https://doi.org/10.1016/j.jvolgeores.2010.03.008.

Morelli, S., V. Pazzi, V. H. Garduño Monroy, and N. Casagli. 2017. "Residual slope stability in low order streams of angangueo mining area (Michoacán, Mexico) after the 2010 Debris flows." In *Advancing culture of living with landslides. Volume 4: Diversity of landslide forms*, edited by M. Mikos, N. Casagli, Y. Yin, and K. Sassa, 651–660. Cham, Switzerland: Springer.

Morelli, S., S. Segoni, G. Manzo, L. Ermini, and F. Catani. 2012. "Urban planning, flood risk and public policy: The case of the Arno River, Firenze, Italy." *Appl. Geogr.* 34 (May): 205–218. https://doi.org/10.1016/j.apgeog.2011.10.020.

Morgenstern, N. R., and V. E. Price. 1965. "The analysis of the stability of general slip surfaces." *Géotechnique* 15 (1): 79–93. https://doi.org/10.1680/geot.1965.15.1.79.

Nakamura, Y. 1989. "A method for dynamic characteristics estimation of subsurface using microtremor on the ground surface." *Q. Rep. Railway Tech. Res. Inst.* 30 (1): 25–33.

Nocentini, M., V. Tofani, G. Gigli, F. Fidolini, and N. Casagli. 2015. "Modeling debris flows in volcanic terrains for hazard mapping: The case study of Ischia Island (Italy)." *Landslides* 12 (5): 831–846. https://doi.org/10.1007/s10346-014-0524-7.

Pandeli, E. 2008. "La pianura di Firenze-Prato-Pistoia nel quadro dell'evoluzione geologica dell'Appennino settentrionale [The plain of Florence-Prato-Pistoia in the framework of the geological evolution of the northern Apennines]." In *Proc., Un piano per la Piana: idee e progetti per un parco*, 1–16. Florence, Italy: Univ. of Florence.

Paolini, F. 2014. *Firenze 1946-2005. Una storia urbana e ambientale [Florence 1946-2005. An urban and environmental history]*. Milan, Italy: FrancoAngeli.

Pazzi, V., A. Lotti, P. Chiara, L. Lombardi, M. Nocentini, and N. Casagli. 2017a. "Monitoring of the vibration induced on the Arno masonry embankment wall by the conservation works after the May 25, 2016 riverbank landslide." *Geoenviron. Disasters* 4 (1): 6. https://doi.org/10.1186/s40677-017-0072-2.

Pazzi, V., S. Morelli, and F. Fanti. 2019. "A review of the advantages and limitations of geophysical investigations in landslide studies." *Int. J. Geophys.* 2019: 27. https://doi.org/10.1155/2019/2983087.

Pazzi, V., S. Morelli, F. Fidolini, E. Krymi, N. Casagli, and R. Fanti. 2016a. "Testing cost-effective methodologies for flood and seismic vulnerability assessment in communities of developing countries (Dajç, northern Albania)." *Geomat. Nat. Haz. Risk* 7 (3): 971–999. https://doi.org/10.1080/19475705.2015.1004374.

Pazzi, V., S. Morelli, F. Pratesi, T. Sodi, L. Valori, L. Gambacciani, and N. Casagli. 2016b. "Assessing the safety of schools affected by geo-hydrologic hazards: The geohazard safety classification (GSC)." *Int. J. Disast. Risk Re.* 15 (Mar): 80–93. https://doi.org/10.1016/j.ijdrr.2015.11.006.

Pazzi, V., L. Tanteri, G. Bicocchi, A. Caselli, M. D'Ambosio, and R. Fanti. 2017b. "H/V technique for the rapid detection of landslide slip surface(s): Assessment of the optimized measurements spatial distribution." In *Advancing culture of living with landslides. Volume 2: Advances in landslide science*, edited by M. Mikos, B. Tiwari, Y. Yin, and K. Sassa, 335–343. Cham, Switzerland: Springer.

Pazzi, V., L. Tanteri, G. Bicocchi, M. D'Ambosio, A. Caselli, and R. Fanti. 2017c. "H/V measurements as an effective tool for the reliable detection of landslide slip surfaces: Case studies of Castagnola (La Spezia, Italy) and Roccalbegna (Grosseto, Italy)." *Phys. Chem. Earth.* 98 (Apr): 136–153. https://doi.org/10.1016/j.pce.2016.10.014.

Pazzi, V., D. Tapete, L. Cappuccini, and R. Fanti. 2016c. "An electric and electromagnetic geophysical approach for subsurface investigation of anthropogenic mounds in an urban environment." *Geomorphology* 273 (Nov): 335–347. https://doi.org/10.1016/j.geomorph.2016.07.035.

Poggi, G. 1882. *Sui lavori per l'ingrandimento di Firenze. Relazione (1864-1877). [On the works for the enlargement of Florence. Report (1864-1877)].* Florence, Italy: Barbera Edizioni.

Raynolds, J. M. 2011. *An introduction to applied and environmental geophysics*. Oxford, UK: Wiley.

Rinaldi, M. 1996. "Variazioni morfologiche recenti dell'alveo del fiume Arno." [Recent morphological changes in the Arno riverbed]. In *Proc., La difesa dalle alluvioni*, 65–79. Perugia, Italy: Gruppo Nazionale per la Difesa dalla Catastrofi Idrogeologiche.

Scampoli, E. 2010. *Firenze, archeologia di una città, secoli I a.C.–XIII d.C. [Florence, archeology of a city, centuries I B.C.–XIII A.D.].* Florence, Italy: Firenze University Press.

Spizzichino, D., C. Margottini, S. Castellaro, and F. Mulargia. 2013. "Passive seismic survey for cultural heritage landslide risk assessment." In *Landslide Science and Practice. Volume 6: Risk Assessment, Management and Mitigation*, edited by C. Margottini, P. Canuti, and K. Sassa, 483–489. Berlin: Springer.

Tapete, D., N. Casagli, G. Luzi, R. Fanti, G. Gigli, and D. Leva. 2013. "Integrating radar and laser-based remote sensing techniques for monitoring structural deformation of archaeological monuments." *J. Archaeol. Sci.* 40 (1): 176–189. https://doi.org/10.1016/j.jas.2012.07.024.

Tapete, D., S. Morelli, R. Fanti, and N. Casagli. 2015. "Localising deformation along the elevation of linear structures: An experiment with space-borne InSAR and RTK GPS on the Roman Aqueducts in Rome, Italy." *Appl. Geogr.* 58 (Mar): 65–83. https://doi.org/10.1016/j.apgeog.2015.01.009.

Tarchi, D., H. Rudolf, G. Luzi, L. Chiarantini, P. Coppo, and A. J. Sieber. 1999. "SAR interferometry for structural change detection: A demonstration test on a dam." In *Vol. 3 of Proc., IEEE 1999 International Geoscience and Remote Sensing Symposium. IGARSS '99 (Cat. No. 99CH36293)*, 1522–1524. Hamburg, Germany: IEEE. https://doi.org/10.1109/IGARSS.1999.772006.

Tarchi, D., H. Rudolf, M. Pieraccini, and C. Atzeni. 2010. "Remote monitoring of buildings using a ground-based SAR: Application to cultural heritage survey." *Int. J. Remote Sens.* 21: 3545–3551. https://doi.org/10.1080/014311600750037561.

Themistocleous, K., C. Danezis, P. Frattini, G. Crosta, and A. Valagussa. 2018. "Best practices for monitoring, mitigation, and preservation of cultural heritage sites affected by geo-hazards: The results of the PROTHEGO project." In Vol. 10773 of *Proc., 6th Int. Conf. on Remote Sensing and Geoinformation of the Environment (RSCy2018)*, 107730Z. Paphos, Cyprus: International Society for Optics and Photonics. https://doi.org/10.1117/12.2503915.

Themistocleous, K., M. Ioannides, A. Agapiou, and D. G. Hadjimitsis. 2015. "The methodology of documenting cultural heritage sites using photogrammetry, UAV, and 3D printing techniques: The case study of Asinou Church in Cyprus." In Vol. 9535 of *Proc., 3rd Int. Conf. on Remote Sensing and Geoinformation of the Environment (RSCy2015)*, 953510. Paphos, Cyprus: International Society for Optics and Photonics. https://doi.org/10.1117/12.2195626.

Tofani, V., G. Bicocchi, G. Rossi, S. Segoni, M. D'Ambrosio, N. Casagli, and F. Catani. 2017. "Soil characterization for shallow landslides modeling: A case study in the Northern Apennines (Central Italy)." *Landslides* 14 (2): 755–770. https://doi.org/10.1007/s10346-017-0809-8.

Travelletti, J., and J.-P. Malet. 2012. "Characterization of the 3D geometry of flow-like landslides: A methodology based on the integration of multi-source data." *Eng. Geol.* 128: 30–48. https://doi.org/10.1016/j.enggeo.2011.05.003.

UNESCO. 1972. *Convention concerning the protection of the world cultural and natural heritage: Adopted by the General conference at its seventeenth session, 16 November 1972*. Paris: UNESCO.

Westoby, M. J., J. Brasington, N. F. Glasser, M. J. Hambrey, and J. M. Reynolds. 2012. "'Structure-from-Motion' photogrammetry: A low-cost, effective tool for geoscience applications." *Geomorphology* 179 (Dec): 300–314. https://doi.org/10.1016/j.geomorph.2012.08.021.